



## Moderate conformational impact of citrate on ovotransferrin considerably increases its capacity to self-assemble at the interface

Cécile Le Floch-Fouéré, Stephane Pezennec, Maryvonne Pasco, Gilles Paboeuf, Anne Renault, Sylvie Beauflis

### ► To cite this version:

Cécile Le Floch-Fouéré, Stephane Pezennec, Maryvonne Pasco, Gilles Paboeuf, Anne Renault, et al.. Moderate conformational impact of citrate on ovotransferrin considerably increases its capacity to self-assemble at the interface. *Journal of Colloid and Interface Science*, 2015, 437, pp.219-226. 10.1016/j.jcis.2014.09.035 . hal-01128555

**HAL Id: hal-01128555**

**<https://hal.science/hal-01128555>**

Submitted on 2 Jul 2015

**HAL** is a multi-disciplinary open access archive for the deposit and dissemination of scientific research documents, whether they are published or not. The documents may come from teaching and research institutions in France or abroad, or from public or private research centers.

L'archive ouverte pluridisciplinaire **HAL**, est destinée au dépôt et à la diffusion de documents scientifiques de niveau recherche, publiés ou non, émanant des établissements d'enseignement et de recherche français ou étrangers, des laboratoires publics ou privés.

Moderate conformational impact of citrate on ovotransferrin considerably increases its capacity to self-assemble at the interface

Cécile Le Floch-Fouéré<sup>\*,a,b</sup>, Stéphane Pezennec<sup>a,b</sup>, Maryvonne Pasco<sup>a,b</sup>, Gilles Paboeuf<sup>a,b</sup>, Anne Renault<sup>c</sup>, Sylvie Beaufigli<sup>c</sup>

<sup>a</sup>INRA, UMR1253 Science et Technologie du Lait et de l'Œuf, F- 35042 Rennes, France

<sup>b</sup>AGROCAMPUS OUEST, UMR1253 Science et Technologie du Lait et de l'Œuf, F-35042 Rennes, France

<sup>c</sup>Institut de Physique de Rennes,

UMR6251 URI-CNRS, Université de Rennes 1, F-35042 Rennes, France

\* Corresponding author. E-mail address: cecile.lefloch@agrocampus-ouest.fr

## Abstract

We have compared the behavior of ovotransferrin at the air-solution interface in the presence of a monovalent ion (acetate), or a divalent ion (citrate), the latter being known to induce conformational changes of this protein upon interaction with its iron-binding sites. We have characterised the adsorption layer at the air-water interface in terms of homogeneity, surface concentration excess and rheological properties at pH 4.0. Besides we have investigated the bulk conformation in the presence of the two anions. In the presence of citrate only, interfacial layers display well-defined domains of higher overall surface concentration suggesting multilayers adsorption. Citrate also induces higher helical content and stabilises the protein against thermal denaturation. Hence we propose that these changes are involved in the propensity of ovotransferrin to self-assemble at the air-water interface resulting in thick and heterogeneous interfacial layer.

**Keywords:** *Protein-ion interaction; Adsorption; Air-water interface; Conformation; Ovotransferrin; multilayers*

## 1. Introduction

Ovotransferrin, also called conalbumin, is a member of the family of iron-binding proteins. It constitutes about 13 % of egg albumen proteins [1] and is a member of the transferrins, soluble glycoproteins implicated in the regulation and transport of iron in vertebrates [2]. It is a protein of known sequence and three dimensional structure [3, 4] whose isoelectric point (pI) is equal to 6.5. Ovotransferrin is a glycoprotein with 686 amino acid residues and a molecular weight of 77700 kDa. It is organized in two lobes of similar conformation (lobe N and lobe C) linked together with a short connecting peptide. Each lobe is made of two domains containing a single high-affinity iron-binding site in the inter-domain cleft, enabling ovotransferrin to exhibit antimicrobial activity through iron deprivation [5,6].

Even if several studies on ovotransferrin as iron-loading and iron-release mechanisms have been devoted, little is known about functional properties of this protein. Yet, egg albumen proteins, are widely used in food industry as foaming agents because of their excellent interfacial properties [7-10]. Consequently, there has been much interest in understanding the relationships between protein structure and interfacial properties [11-15]. In particular, two globular proteins of egg-white, ovalbumin and lysozyme, have been extensively studied at the air–water interface. A large set of data are available about essentially macroscopic aspects of its interfacial behavior like tensioactivity, adsorption kinetics, interfacial shear and dilatational rheology [16-32]. It is not the case of ovotransferrin which is the second most abundant protein in hen egg albumen: as far as we know, no research work has been devoted to its adsorption kinetics at the air-water interface and to the influence of bulk protein concentration on the kinetics.

In a previous work [33], we have investigated the adsorption behavior of apo-ovotransferrin and its interfacial properties at its iso-electric pH (pH 6.5) and in conditions of negative net charge (pH 8.0), in a four-decade concentration range. We have reported that no significant difference was observed between pH 6.5 and 8.0 as regards the final value of surface concentration and surface pressure. However at low concentration, a weak barrier to adsorption is evidenced at pH 6.5. Moreover at a pH where the protein net charge is negative (pH 8.0), the behavior of ovotransferrin at the air–water interface is more influenced by charge effects rather than bulk concentration effects. At this pH, the interface exhibits a low shear viscoelastic constant and a spectral signature not usual for globular proteins.

From these results, directions of further experiments have been proposed to obtain information about the adsorption of ovotransferrin at the air-water interface in conditions of positive

net charge (pH 4.0). In the present work, we describe the effect of two different buffers (same pH and ionic strength) on its adsorption. Several techniques were used to characterize in situ the time evolution of the physical properties and structure of the interfacial films. Ellipsometry and surface pressure measurements allowed us to estimate the amount of protein at the interface and to determine lateral interactions, respectively. On the other hand, surface rheology was used to detect the development of a rigid network at the interface while circular dichroism has allowed study of the conformation change of ovotransferrin in two acid buffers.

## 2. Experimental

### 2.1. Materials

Iron-free ovotransferrin was isolated from hen egg albumen by a two-step chromatographic procedure by using an anion exchanger as already described [34]. Briefly, batches of egg albumen were first diluted with 2 volumes of 20 mM Tris-HCl and the mixture was adjusted to pH 6.0 with 1 M HCl. The precipitated material was discarded by centrifugation and the Tris-egg albumen mixture was adjusted to pH 8.2 with 5 M NaOH, then centrifuged in order to remove insoluble material. Egg-white proteins were separated on a Q-Sepharose Fast Flow anion exchanger (Pharmacia Biotech AB, Saclay, France) column connected to a Biopilot™ system (Pharmacia Biotech AB) equipped with 280 nm UV and conductivity detectors. Bound material was recovered by using an isocratic elution program with a 67 mM sodium phosphate buffer containing 0.5 M NaCl. In a second step, ovotransferrin was further purified by a conventional preparative column chromatography where the bound material was eluted by a linear gradient of NaCl concentrations from 0 to 0.1 M in 120 min. Ovotransferrin fractions were desalted by diafiltration with deionised water and lyophilized.

The effect of two buffers on ovotransferrin was studied at the concentration of 100  $\mu\text{g.mL}^{-1}$  at pH 4.0 at the same ionic strength ( $I \approx 27 \text{ mM}$ ): 20.8 mM sodium citrate and 182 mM sodium acetate.

### 2.2. Ellipsometry, Brewster angle microscopy and surface pressure measurements

The ellipsometric measurements were carried out with a house-made null-ellipsometer operated with He-Ne laser ( $\lambda=632.8 \text{ nm}$ , Melles Griot) polarised with a Glan-Thompson polariser [35]. The ellipsometric angles  $\Delta$ , precision of 0.5 °, and surface pressure  $\Pi$ , precision of

0.5 mN.m<sup>-1</sup>, were recorded simultaneously. The surface pressure was measured using a Wilhelmy plate. The volume of the Teflons sample trough was 8 mL. The protein was diluted in the buffer and poured into the trough directly after preparation. All the experiments were performed at least thrice at room temperature in the range 19–21 °C. The volume of liquid in the sample trough was adjusted to the initial volume by injecting buffer in the subphase with the help of a peristaltic pump which allows following adsorption kinetics over long periods (40 hours) getting rid of the phenomenon of evaporation. In the conditions of Fig. 1 (low bulk protein concentration, early adsorption stages), the surface concentration,  $\Gamma$ , of adsorbed protein was estimated using the measured ellipsometric angle,  $\Delta$ . Figure SI 1 shows that in a small range of  $\Delta$  values, corresponding to the early stages of adsorption at low bulk concentrations, for thicknesses consistent with what has been described for monolayers of other globular proteins [32], the surface concentration  $\Gamma$  can be linearly approximated from the ellipsometric angle  $\Delta$  ( $\Gamma \sim 0.2 \times \Delta$ ). We used this linear estimation for the data of Figure 1. However this estimation cannot be used outside of this low range or when the interfacial layer thickness cannot be assumed to be comparable to the thickness of a globular protein monolayer. Except for the data of Figure 1, which needed to be compared with data from literature, we chose to use raw  $\Delta$  values to compare semi-quantitatively the different adsorption kinetics.

A Brewster angle microscope (BAM) was mounted allowing the visualisation of the surface during the adsorption of the protein [36]. On the same device as for ellipsometry and surface pressure measurements (i.e. on the same air-solution interface) but orthogonally to the ellipsometric optical plane, a CCD camera collected the specular reflection of a *p*-polarized He-Ne laser on the air-solution interface. The incidence of the laser was set to the Brewster angle for the air-water interface, i.e. the incidence for which, according to the Fresnel equations, the *p* polarization (parallel to the incidence plane) is perfectly transmitted through the interface, with no reflection:

$$\theta_{\text{Brewster}} = \arctan(n_{\text{water}} / n_{\text{air}}) \quad (1)$$

with  $n_{\text{water}}$  and  $n_{\text{air}}$  the refraction indices of water and air, respectively  $\theta_{\text{Brewster}}$  approx. 53.11 °). Thus, on pure water, there is no reflected light, and the overall light intensity monitored by the camera is minimal. In the presence of an adsorbed interfacial ovotransferrin layer, the grey-level pattern of the BAM image reflected changes in the interfacial refractive index, i.e. in-plane heterogeneity in the protein adsorbed amount.

### 2.3. Shear viscoelastic constant measurements

The rheometer used [37-39] is based on the action of a very light float applying a rotational strain to the surface through a magnetic couple (with a pair of Helmholtz coils and a small magnet pin deposited in the float). Practically, at the center of a 48 mm diameter Teflon<sup>®</sup> trough, a 10 mm diameter Teflon<sup>®</sup>-coated aluminium disc floats at the air–water interface, surrounded by the surface whose rigidity was measured. The sub-phase was 5 mm deep. The float carries a small magnet and was kept centered in the trough by a permanent field of  $2.10^{-5}$  T, parallel to the Earth's field, created by a small solenoid located just above the float. Sensitive angular detection of the float rotation was achieved using a mirror fixed on the magnet that reflects a laser beam onto a differential photodiode. A sinusoidal torque excitation was applied to the float in the 0.01–100 Hz frequency range, by an oscillating field perpendicular to that of the solenoid. The latter field acts as a restoring torque equivalent to a surface having a  $0.16 \text{ mN.m}^{-1}$  rigidity. On pure sub-phase, this device behaves like a simple harmonic oscillator. Amplitude and phase of the angular response  $\theta$  were measured, and considered to reflect directly the rotational strain of the surface.

For the experimental procedure, the amplitude and phase of the mechanical response of the pure sub-phase was first analysed in the frequency range 0.01-100 Hz to assess that no rigidity was detected and to obtain the eigenpulsation of the system in the absence of visco-elastic interface. This measurement takes approximately one hour. Then, the protein solution was directly poured in the trough and after 20 h of adsorption the complex rotational amplitude was measured as a function of the excitation frequency. A driven, damped harmonic oscillator model was adjusted to the movement of the float and the complex rotational amplitude of the float then is:

$$\theta_0 = (\omega_0^2 \alpha_0) / (\omega_0^2 - \omega^2 + i\gamma \omega) \quad (2)$$

where  $\alpha_0$  is the excitation angle imposed by the magnetic field,  $\omega$  is the pulsation,  $\gamma$  the damping coefficient, and  $\omega_0$  is the eigenpulsation of the system. The complex rotational amplitude is measured as a function of the excitation frequency, and the real and imaginary parts of the model

are both fitted to the data, using the eigenpulsation as a fitting parameter. If the fit is good, it can be asserted that the layer behaves as a visco-elastic layer. In the opposite case, when the visco-elastic model does not fit satisfactorily the data, we can just assert that more complex rheological effects are implied (fractures, creep...). All the experiments were performed at room temperature in the range 19–21 °C.

#### 2.4. Circular dichroism

Circular dichroism (CD) spectra were recorded at 25 °C on a Jasco 810 (Jasco, Bouguenais, France) spectropolarimeter equipped with a thermostatted cell holder. Three spectra recorded at 50 nm.min<sup>-1</sup> were averaged for each sample. Quartz cells with 2 mm light path length were used for measurements. Protein concentrations were 0.77 g.l<sup>-1</sup> for ovotransferrin to obtain absorbance at 280 nm, between 0.8 and 1.0. Far-UV CD-spectra were recorded from 180 to 250 nm with a 0.02 cm light path. Near-UV CD-spectra were recorded from 250 to 330 nm with a 1 cm light path. CD-spectra were expressed in terms of molar ellipticity.

$$[\theta_{\lambda}] = (3300 * \Delta A_{\lambda}) / (C * d) \quad (3)$$

where  $[\theta_{\lambda}]$ , is the molar ellipticity at wavelength  $\lambda$ , expressed in deg.cm<sup>2</sup>.dmol<sup>-1</sup>,  $\Delta A_{\lambda}$  is the difference of absorbance of right- and left-circular polarized light of equal intensity and of the same wavelength  $\lambda$ , C is the mean residue concentration when the far-UV CD-spectrum was reported and the protein molarity in the near UV region, and d (cm) is the light path.

Ovotransferrin charge was calculated with the BioPerl toolkit using the Emboss set of residue pK [42,43].

#### 2.5. Thermal analysis

Differential Scanning Calorimetry (DSC) was used to assess the changes in proteins conformation induced by thermal denaturation [40]. DSC was performed using a Q1000 differential scanning calorimeter (TA Instruments, Paris, France). A volume of 90 µL of protein solution was poured in hermetic stainless steel pans, and water was used as the reference. The heat-up ramp is from 4 to 120 °C at a heating rate of 2 °C.min<sup>-1</sup>. The ovotransferrin peak denaturation temperature,

determined using TA data analysis software, is taken as characteristic value of the denaturation degree, and the overall enthalpy of denaturation is calculated from 50 to 90 °C.

### 3. Results

#### 3.1. In the first steps of adsorption citrate favors interfacial self-assembly

We have compared the very first steps of adsorption by plotting the surface pressure versus surface concentration at the lowest concentration for which the surface pressure is different from zero, i.e 1  $\mu\text{g.mL}^{-1}$  in citrate and 3  $\mu\text{g.mL}^{-1}$  in acetate (Fig. 1). The acquisition frequency of our null-ellipsometry setup is limited to 5-6 measurements per minute. Therefore, the respective adsorption kinetics were adjusted, via the respective concentrations, to observe both surface pressure and surface concentration in the time window where they start to increase.

In the case of diffusion-driven adsorption, Ward and Tordai have shown that the surface concentration varies as the square root of the time  $t$  (Eq. 4) [43]:

$$\Gamma(t) = 2c_0(Dt/\pi)^{1/2} \quad (4)$$

where  $D$  is the diffusion coefficient, from the bulk to the interface. Therefore, the initial part of the  $\Gamma$  versus  $t^{1/2}$  plot at low concentrations should be linear and the diffusion coefficient can be extracted experimentally. However, when an energy barrier is present, the measured diffusion coefficient extracted from the linear regime is an apparent one [28]. Nevertheless, this parameter allows a comparison between proteins and is usually found in the  $10^{-11} \text{ m}^2.\text{s}^{-1}$  range for small objects in solution. This linear regime was actually observed for ovotransferrin at pH 4.0 in citrate at 1  $\mu\text{g.mL}^{-1}$  and in acetate at 3  $\mu\text{g.mL}^{-1}$  (Fig. SI 2), and the  $D$  values were  $6.59 \times 10^{-11}$  and  $9.47 \times 10^{-11} \text{ m}^2.\text{s}^{-1}$ , respectively.



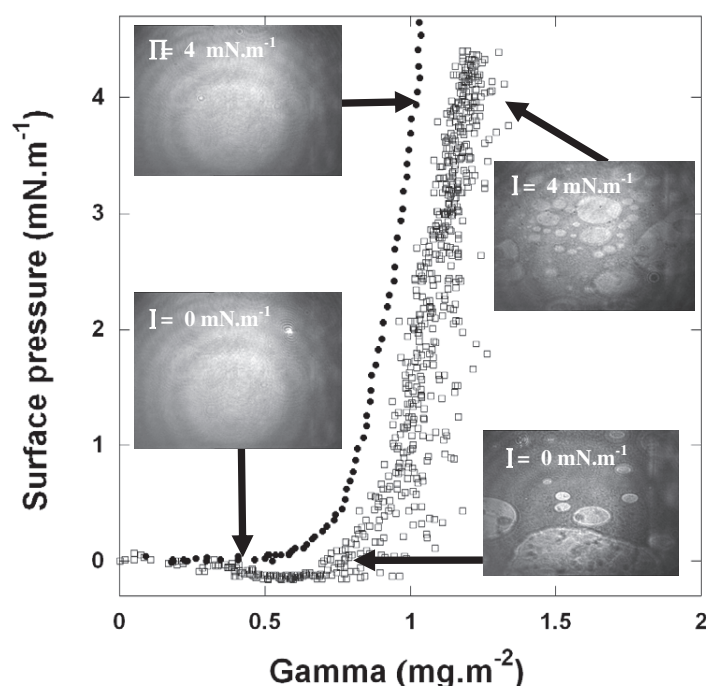


**Fig. 1.** Surface pressure ( $\Pi$ ) versus surface concentration ( $\Gamma$ ) for the lowest subphase concentrations for which the surface pressure is initiated:  $1 \mu\text{g.mL}^{-1}$  for ovotransferrin in citrate (open squares) and  $3 \mu\text{g.mL}^{-1}$  in acetate (filled circles). The insert in the BAM pictures ( $430 \times 540 \mu\text{m}^2$ ) shows the images of the surface for a pressure equal to  $0 \text{ mN.m}^{-1}$  and  $4 \text{ mN.m}^{-1}$

Fig. 1 shows for ovotransferrin in the presence of citrate an initial decrease in surface pressure prior the expected final increase, while no decrease is observed for ovotransferrin in acetate. This point will be detailed further in the discussion section.

The plot of surface pressure versus surface concentration for low subphase concentration allows to extract two parameters relevant for the description of the very first steps of adsorption. First, the minimum surface concentration,  $\Gamma_0$ , necessary to initiate surface pressure is related to the extent of cohesive interactions between the adsorbed molecules [44]. Values of  $\Gamma_0$  in citrate and in acetate are similar ( $0.92$  and  $0.78 \text{ mg.m}^{-2}$  respectively) which is consistent with values of several proteins lie between  $0.1$  and  $1.2 \text{ mg.m}^{-2}$  [44]. It is the case for ovotransferrin at pH 6.5 and at pH 8.0 ( $0.77$  and  $0.45 \text{ mg.m}^{-2}$  respectively) [33].

The second parameter extracted from Fig. 1 is  $\theta$ , the instantaneous surface pressure increase as a result of adsorption of  $1 \text{ mg}$  of protein per  $\text{m}^2$ . This parameter has a value of around  $13.0 \text{ mN.m.mg}^{-1}$  for ovotransferrin at pH 4.0 in the two buffers, that is consistent with those of literature for bovine  $\beta$ -casein and caprine  $\alpha_{s1}$ -casein ( $9.0$  and  $12.0 \text{ mN.m.mg}^{-1}$ , respectively) [45].

This  $\theta$  value is twice as ovotransferrin at pH 8.0 and 6.5, indicating that at pH 4.0, indicating that the magnitude of interactions in the interfacial film is rather strong in the first steps of adsorption [44].

The adsorption kinetics were also followed by Brewster angle microscopy to observe the formation of the film at the air-water interface. BAM images were performed at different stages of adsorption and especially when the surface pressure is equal to 0 and 4.0 mN.m<sup>-1</sup> as shown inserts in Figure 1. The image resolution is of the order of microns. On the adsorption of ovotransferrin at 3 µg.mL<sup>-1</sup> in acetate, no domain is observed which indicates a very homogeneous film at the micrometer scale. In contrast, the films formed for ovotransferrin at 1 µg.mL<sup>-1</sup> in citrate show a strong heterogeneity with domains observed from the first moments of the adsorption. We can see a coexistence of heterogeneous liquid condensed (circular domains) and homogeneous liquid expanded domains (dark image).

### 3.2. Interfacial heterogeneity in the presence of citrate

Adsorption kinetics were also monitored by ellipsometry for 40 h for a bulk concentration of 100 µg.mL<sup>-1</sup> at pH 4.0 in citrate and acetate. Fig. 2 shows plots of the ellipsometric angle  $\Delta$  as a function of the adsorption time for these two buffers.

At pH 4.0 in acetate, kinetics of adsorption for a bulk ovotransferrin concentration of 100 µg.mL<sup>-1</sup> are typical for globular proteins and comparable with those obtained with ovalbumin [22] and ovotransferrin [33]. A final plateau value close to 12° is rapidly reached during the adsorption kinetics which is consistent with the formation of a saturated monolayer [22,26,31,41,42].

At pH 4.0 in citrate, there is a large variability in the data set. Fig. 2 shows a shaded area corresponding to the variability of 11 kinetics obtained for ovotransferrin in this buffer. Values of the angle  $\Delta$ , which reflects the surface concentration excess, vary from one to three after 40 h (from 17 to 52 °). Two of the eleven kinetics are similar to those obtained with acetate reminiscent monolayers while the nine others have very high values of delta. In that case, the fact that the  $\Delta$  value of ovotransferrin is much higher than the expected  $\Delta$  value for a monolayer of a protein suggests that multilayers are formed at the air–water interface. Moreover, in many cases, the ellipsometric angle, did not reach stabilized values and kept on increasing for hours. Our interpretation will be detailed in the discussion section.

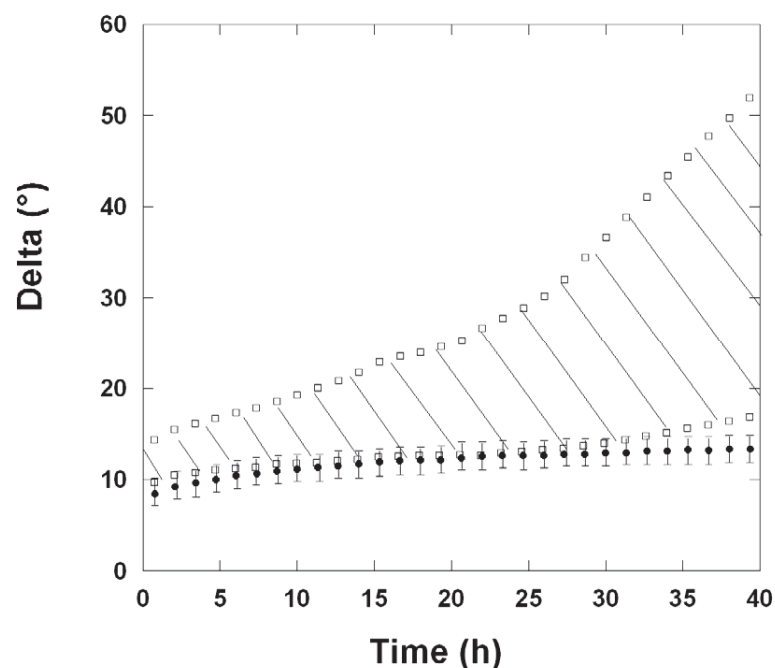


**Fig. 2.** Adsorption kinetics followed by ellipsometry measurements during 40 hours for a bulk concentration of  $100 \mu\text{g.mL}^{-1}$  at pH 4.0 in citrate (open squares) and acetate (filled circles). The shaded area corresponds to the variability of 11 kinetics obtained for the ovotransferrin in citrate.

Adsorption kinetics have also been studied with surface pressure measurements. Fig. 3 shows the surface pressure versus time at pH 4.0 with the two buffers for a bulk concentration of ovotransferrin of  $100 \mu\text{g.mL}^{-1}$ . In these two buffers, surface pressure showed a saturating profile, typical for surface-active globular proteins with plateau values in the  $20\text{--}22 \text{ mN.m}^{-1}$  range (Fig. 3). For comparison, values obtained for ovotransferrin at pH 6.5 and 8.0 at this concentration are close to  $18 \text{ mN.m}^{-1}$  [33]. However, if the final value is the same, kinetics of surface pressure are different on shorter time. Inset in Fig. 3 shows adsorption during 2 hours in citrate and acetate. The pressure values are higher in the early moments of kinetics in the case of ovotransferrin at pH 4.0 in citrate indicating that the ovotransferrin layer is organized more quickly to the air-water interface in this buffer.

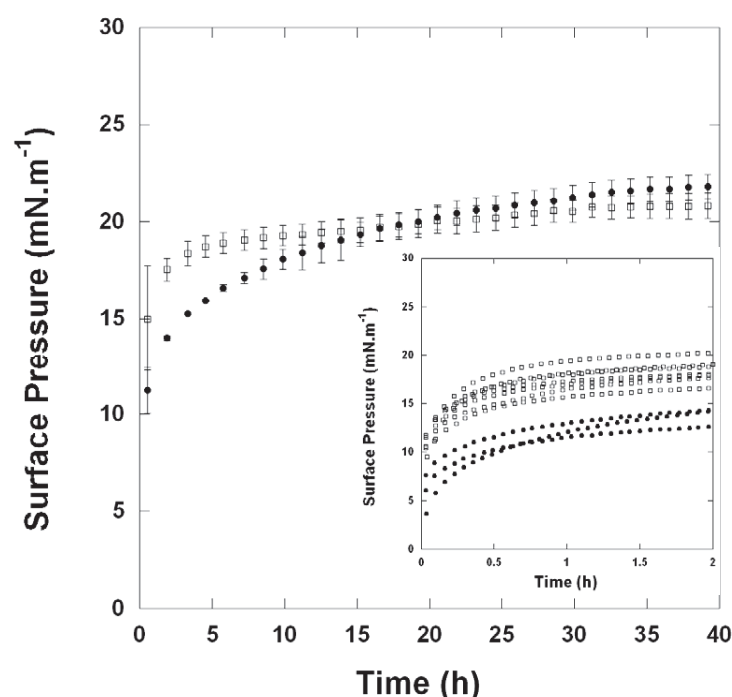


**Fig. 3.** Surface pressure versus adsorption time (40 hours) for a bulk concentration of  $100 \mu\text{g.mL}^{-1}$  at pH 4.0 in citrate (open squares) and acetate (filled circles). Inset shows adsorption during 2 hours in citrate (open squares) and acetate (filled circles)

### 3.3. In the presence of citrate the interfacial layer is not viscoelastic

In parallel to the ellipsometry measurements, we have carried out rheology measurements with a set-up dedicated to the study of viscoelastic interfacial layers. The mechanical response of the layer has been measured as a function of the excitation frequency after 20 h of adsorption. This time was chosen to take into account the time scale of protein rearrangements in the interfacial layer. A fit of the data (real and imaginary parts of the rotational amplitude of the float) using an viscoelastic model (Fig. 4a,b, solid line) has allowed to determine whether the films behave like a viscoelastic film or if more complex rheological effects are involved. An increase in the shear viscoelastic constant is reflected by a shift of the curves towards high frequencies. Typical behaviors for ovotransferrin at  $100 \mu\text{g.mL}^{-1}$  in citrate and acetate are shown in Fig. 4a,b.

These surface rheology measurements show that at a bulk concentration of ovotransferrin at  $100 \mu\text{g.mL}^{-1}$  in acetate (Fig.4b), a viscoelastic model fits adequately the rheological response of ovotransferrin films, which is consistent with a viscoelastic interfacial layer. On the contrary to

ovotransferrin at  $100 \mu\text{g.mL}^{-1}$  in citrate (Fig.4a) for which the viscoelastic model does not fit the mechanical response.

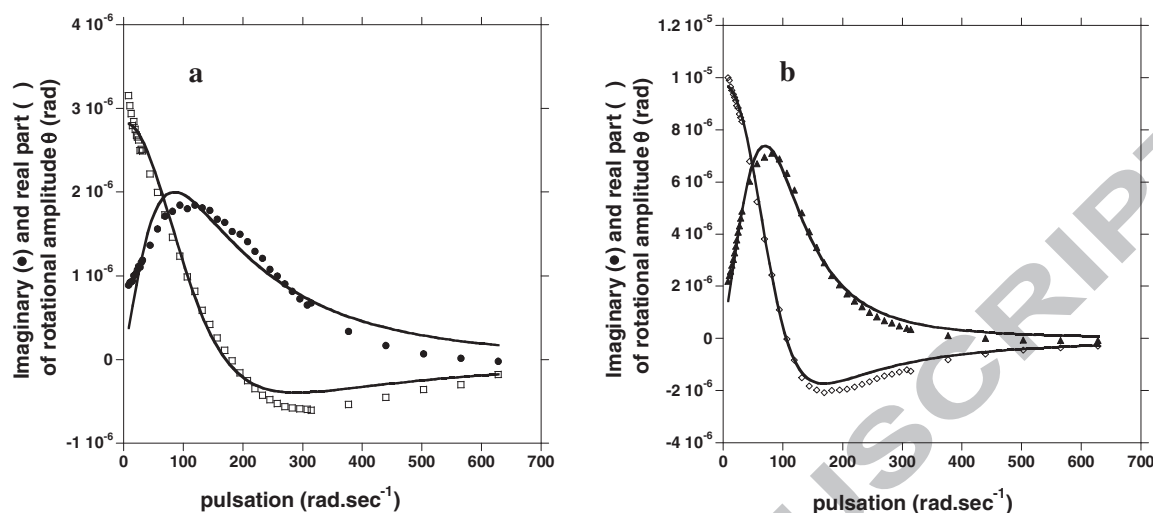


**Fig. 4.** Amplitude of the rotational motion of the float as a function of excitation pulsation, measured 20 h after the beginning of the adsorption of ovotransferrin at a bulk concentration of  $100 \mu\text{g.mL}^{-1}$  in citrate (a) and acetate (b)

### 3.4. Citrate slightly increases helical content and affects the tertiary structure

We have also studied circular dichroism spectroscopy of ovotransferrin in two acid buffers. Far-UV CD spectra enabled us to evaluate the protein secondary structure (Fig.5a) and any change in the environment of aromatic residues and disulfide bonds results in a modification of the near-UV CD spectra (Fig.5b).

Far-UV is used to study the change of secondary structure of secondary structure of ovotransferrin by monitoring the peaks of the corresponding  $\alpha$ -helix and  $\beta$ -sheet. It is known that, when a protein essentially existed in the  $\alpha$ -helical conformation, two negatives bands at  $\sim 209$  nm and  $\sim 222$  nm, and a positive band at  $\sim 190$  nm are observed [46,47,48]. On the other hand, for the existence of a  $\beta$ -sheet, a positive and negative band appeared at 190 and 215 nm, respectively [49,50].

The CD-spectrum of ovotransferrin in citrate has broad negative ellipticity at 209 and 223 nm (to a lesser extent) together with two positive maximum (very noisy spectra) at  $\sim 193$  and  $\sim 199$  nm. These results suggest that the structure of ovotransferrin in this buffer is predominately  $\alpha$ -helical. On the other hand, our CD data show, at pH 4.0 in acetate, a decreasing in negative ellipticity with three small peaks around 201, 212 and 217 nm and a positive maximum at  $\sim$

193 nm. This decrease in intensity of the bands around 209 and 222 nm suggests a lower proportion of  $\alpha$ -helices in this case. Consequently, the protein secondary structure of ovotransferrin in the two buffers is not exactly the same.

CD spectra in near UV region were used to examine the potential effect of two different buffers on tertiary structure of ovotransferrin. The near UV spectra of ovotransferrin in citrate and in acetate reveal three negative ellipticity peaks at around 277, 285 and 296 nm and single shoulder at 291 nm. These results are in agreement with those obtained in the literature to the native state of ovotransferrin [7,51]. As can be observed, the peaks at 277, 285 and 291 nm tend to diminish. The structural changes observed at 277, 285 and 291 nm could be attributed to aromatic amino acid Phe, Tyr and Trp environment [51]. Consequently, the decrease in the peak intensity in acetate reflects subtle changes in the tertiary structure affecting the environment of aromatic amino acid.

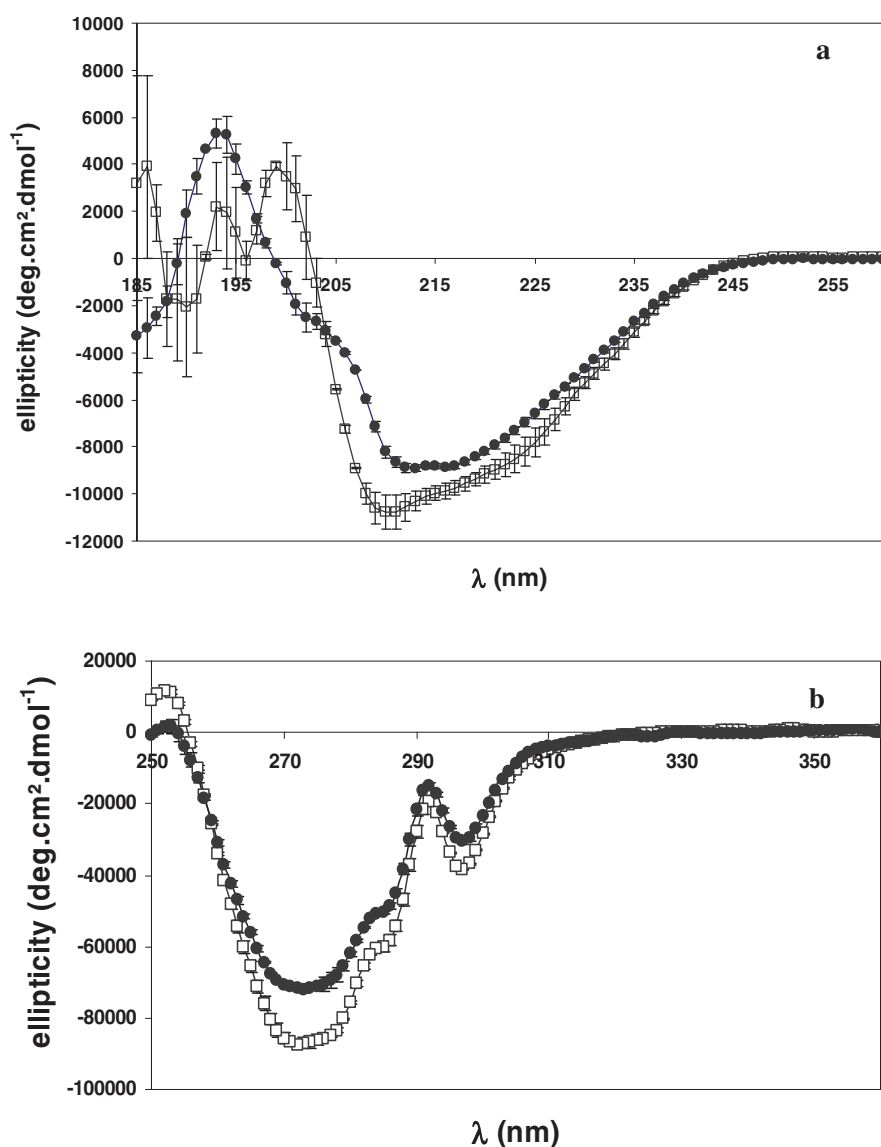


**Fig. 5.** Far- (a) and near- (b) UV CD-spectra of ovotransferrin in citrate (open squares) and in acetate (filled circles) at pH 4.0

### 3.5. Citrate stabilizes ovotransferrin against thermal denaturation

Differential Scanning Calorimetry (DSC) was used to assess the changes in proteins conformation induced by thermal denaturation. The lower scan in Fig.6 was obtained on ovotransferrin in citrate and shown a single peak centered near 81.3 °C. Ovotransferrin in acetate is also detailed in the upper trace in Fig.6 where a single peak centered near 77.4 °C is seen.

Therefore in solution, we can conclude that ovotransferrin is stabilized in the presence of citrate (highest denaturation temperature observed).

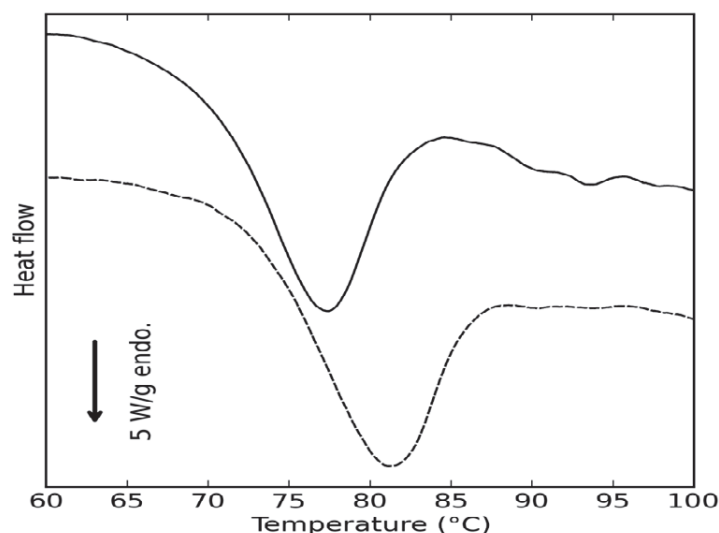


**Fig. 6.** DSC scans on ovotransferrin in citrate (lower trace) and in acetate (upper trace) at pH 4.0. For clarity, DSC traces in this figure have been arbitrarily shifted on the ordinate scale

#### 4. Discussion

The present study was undertaken to characterize the properties of the interfacial film formed by adsorption of ovotransferrin in two different acid buffers (same pH and ionic strength). Complementary techniques have been coupled such as null ellipsometry, which probes up to a thickness of about 100 nm, surface tension which is sensitive to the very first layer, shear viscoelastic constant which reflects the macroscopic mechanical properties of the interfacial film, as thermal and structural analyses to acquire conformational information.

At low initial concentration, ovotransferrin adsorption, as measured by ellipsometry, is diffusion-driven. Below the critical surface concentration  $\Gamma_0$ , where no measurable surface pressure is detected, the average distance between molecules might be too high to allow interactions. Regardless of the buffer used, values of  $\Gamma_0$  are close to 0.8-0.9 mg.m<sup>-2</sup>. These results suggest that ovotransferrin needs as much matter at the interface in citrate or in acetate to initiate lateral interactions. We also observed the same trend for the values of  $\Theta$ , the instantaneous surface pressure increase upon adsorption of 1 mg of protein per m<sup>2</sup>. However, we can observe that in the presence of citrate, a weak barrier to adsorption is revealed by the first decrease of the surface



pressure before the usual increase of the surface pressure with the surface concentration. This phenomenon, known as the “image charge effect” has been mentioned by others [29,42,52-56]. This barrier effect was already observed for ovotransferrin at pH 6.5 but non-existent at pH 8.0 [33]. Sengupta et al. [29] showed that generally, negatively charge proteins exhibit an attraction toward the air-water interface contrarily for positively charged proteins which face up to an energy barrier for their adsorption. This seems to be the case for ovotransferrin in citrate at pH 4.0 where the global net electric charge is equal to +55. However it is quite surprising not to have the same behavior for ovotransferrin in acetate as its net charge is the same. This difference was also noticed thanks to Brewster angle microscopy. The interfacial films in citrate show a strong heterogeneity with circular domains of heterogeneous liquid condensed revealing an increased assembly capacity from the first moments of the adsorption contrary to the ovotransferrin behavior in acetate. These observations seem to suggest a potential impact of ions on ovotransferrin which will be discussed in detail later.

At  $100 \mu\text{g.mL}^{-1}$ , the ellipsometric angle  $\Delta$  as a function of the adsorption time also shows some differences between the two buffers. In acetate, the value of protein surface concentration is about  $2.5 \text{ mg.m}^{-2}$  which is close to the expected value at saturation for apo-ovotransferrin considering its molecular dimensions ( $10 \times 6 \times 5 \text{ nm}^3$ ) [57]. In citrate, there is a large variability in the data set with values of  $\Delta$  from  $17$  to  $52^\circ$  which are much higher than the expected value for this protein. This variability could be interpreted as an experimental lack of reproducibility. However, we exclude this hypothesis, for this behavior was only observed in the presence of citrate, while reproducible kinetics were systematically obtained in the presence of acetate, as for other proteins [16,17]. We think that this variability of the kinetics in the presence of citrate reflects in-plane heterogeneity of the interface, as suggested by the domain formation shown by BAM images in the early stages of adsorption. Thus, when the interfacial layer shows local variations of the adsorbed protein amount, the tiny laser footprint (at most a few square millimeters) isolates a very local  $\Delta$  value which cannot be considered as a representative average of the whole interface. The kinetics with the highest  $\Delta$  values, which are the most frequent ones, were most probably obtained when the laser illuminated "dense", multilayer domains. On the other hand, kinetics with the smallest  $\Delta$  values were obtained when the laser illuminated the monolayer background.

In the present work, a difference has also been observed with kinetics of surface pressure on shorter time. Indeed, in citrate the ovotransferrin layer is organized more quickly to the air-water interface in this buffer. If the pressure values are higher in the early moments of kinetics in the case of citrate, it is not the case for final values (around  $21 \text{ mN.m}^{-1}$ ) typical for globular proteins [31,33,58-62]. This result suggests that the in-plane organization of ovotransferrin is identical

regardless of the type of buffer, while proteins in the sub-subphase seem to assemble differently with increased capacity of assembly in the presence of citrate.

Several studies have shown the interest of the combined use of ellipsometry, surface pressure and shear viscoelastic constant measurements [16,37,39,60,63]. In the present case, our findings suggest that the ovotransferrin film in acetate exhibits a high viscoelasticity which is not the case for the ovotransferrin film in citrate. This not purely viscoelastic behavior has already been observed in previous work for lysozyme, another major protein of egg albumen, which forms multilayers under specific conditions [16]. The rheological surface properties are considered to depend on rearrangements of protein structure within the film [64]. In our experimental conditions, at pH 4.0, citrate owns between one or two negative charges ( $pK_{a1} = 3.13$ ,  $pK_{a2} = 4.76$ ,  $pK_{a3} = 6.40$ ) and acetate between zero and one negative charge ( $pK_a = 4.76$ ). A possible hypothesis would be that the citrate creates electrostatic bridges between the molecules of ovotransferrin to allow an attractive assembly process. This is in agreement with the statement of Graham and Phillips [65] that in addition to the contribution of intermolecular associations, the intramolecular cohesion, i.e. the residual native structure of adsorbed globular proteins plays a significant role in the rheological properties of interfacial films.

In order to study secondary and tertiary structure of ovotransferrin in these two acid buffers, experiments of far-UV CD and near-UV CD were performed. Our results suggest that ovotransferrin conformation in the interfacial film is not exactly the same in the two buffers. Indeed the CD-spectrum of ovotransferrin in citrate suggests that the structure of ovotransferrin in this buffer is predominately  $\alpha$ -helical, whereas in acetate, the CD-spectrum suggests a lower proportion of  $\alpha$ -helices. In its native form, apo-ovotransferrin owns a secondary structure with 25 % helices and 11 %  $\beta$ -sheets (PDB ID 1aiv) [66]. In the case of citrate, our data (far- and near-UV CD) are consistent with those obtained for the native form, especially studied by Lechevalier et al. [7,8] and Rabbani et al. [51], this is quite surprising in an acid pH. This trend is confirmed by DSC measurements where ovotransferrin is stabilized in the presence of citrate (highest denaturation temperature observed). In acetate, our results can be compared with those obtained by Rabbani et al. [51] in the same experimental conditions. These authors showed ovotransferrin existed exclusively as a pre-molten globule state at pH 4.0 in sodium acetate. In fact under acidic conditions, ionisable side chains of the protein get protonated which facilitates the formation of a pre-molten globule or molten globule state, caused by a resultant charge-charge repulsion which consequently leads to protein unfolding and formation of acid-denatured state [67,68].

The transferrins, which include ovotransferrin, are a class of iron-binding proteins that require the presence of carbonate, a synergistic anion. Other anions, particularly small carboxylic acids can also function as synergistic anions in the absence of carbonate [69,70]. Several studies on ovotransferrin as iron-loading and iron-release mechanisms have been devoted. Recently, a review written by Harris [71] detailed the binding of anions to the apoprotein as well as the formation and structure of Fe-anion-transferrin ternary complexes. Other inorganic anions are able to bind to apo-ovotransferrin including sulfate and phosphate [72-75] and to modify the temperature  $T_m$  causing aggregation of ovotransferrin. This is also the case for citrate which could raise temperature  $T_m$  of ovotransferrin about 5-7 °C at neutral pH [76]. At pH 4.0 in citrate value of  $T_m$  is close to  $T_m$  in the diferric form (82 °C at pH 7.5) [77]. When ovotransferrin binds iron thanks to its active sites, it gives rise to a conformational change and increases resistance heating [77,78]. The same tendency has been observed with addition of aluminium at neutral pH [79]. In this work, even if the presence of citrate increases  $T_m$ , it seems not to change secondary or tertiary structure. Oe et al. [74] observed that the anion-binding (especially citrate) markedly protected the N-terminal half molecule from trypsin digestion and disulfide reduction by DTT, and yet no difference in CD spectra was seen between in the presence and absence of an anion. Therefore, despite moderate conformational changes between ovotransferrin in citrate and in acetate, different interfacial behaviors are observed, particularly with fluctuating adsorption in citrate with multilayers. It is interesting to note the only difference between the two buffers (same pH and ionic strength) lies in the nature of ions. According to Harris et al. [80], a dinegative charge appears to be the most important criterion for anion binding which is not the case of acetate. Therefore besides the hypothesis of electrostatic bridging mentioned above, the hypothesis of conformational impact of citrate binding must also be kept in mind.

## 5. Conclusion

Identification of the key physicochemical parameters of proteins that determine their interfacial properties is still incomplete and represents a real stake challenge, especially for food proteins. In a former study [81] we showed that very small structural changes are sufficient to affect strongly the air-water interfacial behavior of globular protein: a physical treatment such as dry heating of lysozyme dramatically increases its propensity to self-assemble. In the present work, we show that citrate ions induce moderate conformational changes of apo-ovotransferrin. Hence we propose that these changes are involved in the propensity of ovotransferrin to self-assemble at the air-water interface resulting in thick and heterogeneous interfacial layer. In contrast, in the presence

of acetate, apo-ovotransferrin adsorbs at the air-water interface, producing a single molecule layer with mechanical properties similar to those of other globular protein systems.

## References

- [1] E.C.Y. Li-Chan, W.D. Powrie, S. Nakai, in: W.J. Stadelman, O.J. Cotterill (Eds), *Egg science and technology*, The Haworth Press, Westport, 1986, p.105.
- [2] P. Aisen, in: T.M. Loehr (Eds), *Physical bioinorganic chemistry*, VCH Publishers, New York, 1989, p.353.
- [3] J-M. Jeltsch, P. Chambon, *Eur. J. Biochem* 122 (1982) 291.
- [4] H. Kurokawa, B. Mikami, M. Hirose, *J. Mol. Biol.* 254 (1995) 196.
- [5] P. Valentini, G. Antonini, C. Von Hunolstein, P. Visca, N. Orsi, E. Antonini, *Int. J. Tissue React.* 5 (1983) 97.
- [6] H.R. Ibrahim, E. Iwamori, Y. Sugimoto, T. Aoki, *Biochim. Biophys. Acta* 1401 (1978) 289.
- [7] V. Lechevalier, T. Croguennec, S. Pezennec, C. Guerin-Dubiard, M. Pasco, F. Nau, *Food Chem.* 92 (2005) 79.
- [8] V. Lechevalier, T. Croguennec, S. Pezennec, C. Guerin-Dubiard, M. Pasco, F. Nau, *J. Agric. Food Chem.* 51 (2003) 6354.
- [9] Y. Mine, *Trends Food Sci. Tech.* 6 (1995) 225.
- [10] T.M. Johnson, M.E. Zabik, *J. Food Sci.* 46 (1981) 1231.
- [11] H. J. de Jongh, H. A. Kusters, E. Kudryashova, M.B.J. Meinders, D. Trofimova, P.A. Wierenga, *Biopolymers* 74 (2004) 131.
- [12] A.H. Martin, K. Grolle, M.A. Bos, M.A.C. Stuart, T. van Vliet, *J. Colloid Interface Sci.* 254 (2002) 175.
- [13] J. McGuire, C.K. Bower, M.K. Bothwell, *Australian Journal of Dairy Technology* 55 (2000) 65.
- [14] M. Hammershaj, A. Prins, K.B. Qvist, *J. Sci. Food Agric.* 79 (1999) 859.
- [15] E. Dickinson, *Colloids Surf. B Biointerfaces* 15 (1999) 161.
- [16] C. Le Floch-Fouéré, S. Pezennec, V. Lechevalier, S. Beaufils, B. Desbat, M. Pézolet, A. Renault, *Food Hydrocolloids* 23 (2009) 352.

- [17] C. Le Floch-Fouéré, S. Beaufils, V. Lechevalier, F. Nau, M. Pézolet, A. Renault, S. Pezennec, *Food Hydrocolloids* 24 (2010) 275.
- [18] A.W. Perriman, J.W. White, *Physica B: Condensed Matter* 385-386 (2006) 716.
- [19] A. Renault, S. Pezennec, F. Gauthier, V. Vié, B. Desbat, *Langmuir* 18 (2002) 6887.
- [20] G. Kim, M. Gurau, J. Kim, P.S. Cremer, *Langmuir* 18 (2002) 2807.
- [21] L. Razumovsky, S. Damodaran, *J. Agric. Food Chem.* 49 (2001) 3080.
- [22] S. Pezennec, F. Gauthier, C. Alonso, F. Graner, T. Croguennec, G. Brulé, A. Renault, *Food Hydrocolloids* 14 (2000) 463.
- [23] J.R. Lu, T.J. Su, B.J. Howlin, *J. Phys. Chem. B* 103 (1999) 5903.
- [24] J.R. Lu, T.J. Su, R.K. Thomas, J. Penfold, J.R.P. Webster, *J. Chem. Soc. Faraday Trans.* 94 (1998) 3279.
- [25] S. Damodaran, K. Anand, L. Razumovsky, *J. Agric. Food Chem.* 46 (1998) 872.
- [26] J. Benjamins, E. H. Lucassen-Reynders, in: D. Möbius, R. Miller (Eds.) *Proteins at liquid interfaces*, Elsevier, Amsterdam, 1998, p.341.
- [27] K. Anand, S. Damodaran, *J. Colloid Interface Sci.* 176 (1995) 63.
- [28] S. Xu, S. Damodaran, *Langmuir* 10 (1994) 472.
- [29] S. Xu, S. Damodaran, *Langmuir* 8 (1992) 2021.
- [30] S. Xu, S. Damodaran, *J. Colloid Interface Sci.* 159 (1993) 124.
- [31] J.A. de Feijter, J. Benjamins, in: E. Dickinson (Ed), *Food emulsions and foams*, Royal Society of Chemistry, London, 1987, p.72.
- [32] J.A de Feijter, J. Benjamins, F.A. Veer, *Biopolymers* 17 (1978) 1759.
- [33] C. Le Floch-Fouéré, S. Pezennec, M. Pézolet, J.F. Rioux-Dubé, A. Renault, S. Beaufils, *J. Colloid Interface Sci.* 356 (2011) 614.
- [34] T. Croguennec, F. Nau, S. Pezennec, M. Piot, G. Brulé, *Eur. Food Res. Technol.* 212 (2001) 296.
- [35] B. Berge, A. Renault, *Europhys. Lett.* 21 (1993) 773.
- [36] S. Henon, J. Meunier, *Review of Scientific Instruments* 62 (1991) 936.
- [37] C. Venien-Bryan, P-F. Lenne, C. Zakri, A. Renault, A. Brisson, J-F. Legrand, B. Berge, *Biophys. J.* 74 (1998) 2649.
- [38] C. Zakri, A. Renault, B. Berge, *Physica B* 248 (1998) 208.

- [39] A. Renault, P-F. Lenne, C. Zakri, A. Aradian, C. Venien-Bryan, F. Amblard, *Biophys. J.* 76 (1999) 1580.
- [40] V.R. Harwalkar, C.-Y. Ma, *Thermal analysis: principles and applications*, S. Nakai, H.M. Modler (Eds.), *Food proteins: Properties and characterization*, VCH Publishers, New York, USA (1996), p. 405.
- [41] D.E. Graham, M.C. Phillips, *J. Colloid Interface Sci.* 70 (1979a) 403.
- [42] T. Sengupta, L. Razumovsky, S. Damodaran, *Langmuir* 15 (1999) 6991.
- [43] A.F.H. Ward, L. Tordai, *J. Chem. Phys.* 14 (1946) 453.
- [44] L. Razumovsky, S. Damodaran, *Langmuir* 15 (1999) 1392.
- [45] S. Beaufils, R. Hadaoui-Hammoutene, V. Vie, G. Miranda, J. Perez, E. Terriac, G. Henry, M-M. Delage, J. Leonil, P. Martin, A. Renault, *Food Hydrocolloids* 21 (2007) 1330.
- [46] Z.W. Yu, J. Jin, Y. Cao, *Langmuir* 18 (2002) 4530.
- [47] M. Kanthimathi, R. Maeshhwari, A. Dhathathreyan, *Langmuir* 19 (2003) 3398
- [48] S.M. Kelly, T.J. Jess, N.C. Price, *Biochimica et Biophysica Acta* 1751 (2005) 119
- [49] J. Zheng, C.A. Constantine, V.K. Rastogi, T.C. Cheng, J.J. DeFrank, R.M. Leblanc, *J. Phys. Chem. B* 108 (2004) 17238
- [50] J. Li, Y. Du, P. Boullanger, L. Jiang, *Thin Solid Films* 352 (1999) 213
- [51] G. Rabbani, E. Ahmad, N. Zaidi, R.H. Khan, *Cell Biochem Biophys* 61 (2011) 551
- [52] S. Beaufils, J.G. Grossmann, A. Renault, V.M. Bolanos-Garcia, *J. Phys. Chem. B* 112 (2008) 7984.
- [53] S. Damodaran, S. Xu, *J. Colloid Interface Sci.* 178 (1996) 426.
- [54] K.B. Song, S. Damodaran, *Langmuir* 7 (1991) 2737.
- [55] P.A. Wierenga, M.B.J. Meinders, M.R. Egmond, A.G.J. Voragen, H.H.J. De Jongh, *J. Phys. Chem. B* 109 (2005) 16946.
- [56] S.S. Datwani, K.J. Stebe, *J. Colloid Interface Sci.* 219 (1999) 282.
- [57] P.A. Wierenga, H. Gruppen, *Curr. Opin. Coll. Interface Sci.* 15 (2010) 365.
- [58] D.E. Graham, M.C. Phillips, *J. Colloid Interface Sci.* 70 (1979b) 415.
- [59] J.E. Stajich, D. Block, K. Boulez, S.E. Brenner, S.A. Chervitz, C. Dagdigian, G. Fuellen, J.G.R. Gilbert, I. Korf, H. Lapp, H. Lehtväslaiho, C. Matsalla, C.J. Mungall, B.I. Osborne, M.R. Pocock, P. Schattner, M. Senger, L.D. Stein, E. Stupka, M.D. Wilkinson, E. Birney, *Genome Res.* 12 (2002) 1611.

- [60] B.S. Murray, in: E. Dickinson (Ed.), Food emulsions and foams, Royal Society of Chemistry, London, 1987, p.170.
- [61] A. Kato, N. Tsutsui, N. Matsudomi, K. Kobayashi, S. Nakai, *Agric. Biol. Chem.* 45 (1981) 2755.
- [62] N. Kitabatake, E. Doi, *J. Food Sci.* 53 (1988) 1542.
- [63] S. Beaufils, R. Hadaoui-Hammoutene, V. Vie, G. Miranda, J. Perez, E. Terriac, G. Henry, M-M. Delage, J. Leonil, P. Martin, A. Renault, *Food Hydrocolloids* 21 (2007) 1330.
- [64] E. Dickinson, B.S. Murray, G. Stainsby, In E. Dickinson & G. Stainsby (Ed.), *Advances in food emulsions and foams*, Elsevier Applied Science, London, 1988, pp. 123–162.
- [65] D.E. Graham, M.C. Phillips, *J. Colloid Interface Sci.* 70 (1979c) 427.
- [66] W. Kabsch, C. Sander, *Biopolymers* 22 (1983) 2577.
- [67] A.L. Fink, L.J. Calciano, Y. Goto, T. Kurotsu, D.R. Palleros, *Biochemistry* 33 (1994) 12504.
- [68] C.N. Pace, R.W. Alston, K.L. Shaw, *Protein Science* 9 (2000) 1395.
- [69] M.R. Schlabach, G.W. Bates, *J. Biol. Chem.* 250 (1975) 2182.
- [70] J. Dubach, B.J. Gaffney, K. More, G.R. Eaton, *Biophys. J.* 59 (1991) 1091.
- [71] W.R. Harris, *Biochim. Biophys. Acta* 1820 (2012) 348.
- [72] R. Nakamura, I. Omori, *Agric. Biol. Chem.* 43 (1979) 2393.
- [73] W.R. Harris, *Biochemistry* 24 (1985) 7412.
- [74] H. Oe, N. Takahashi, E. Doi, M. Hirose, *J. Biochem.* 106 (1989) 858.
- [75] K. Mizutani, H. Yamashita, B. Mikami, M. Hirose, *Biochemistry* 39 (2000) 3258.
- [76] K. Mizutani, Y. Chen, H. Yamashita, M. Hirose, S. Aibara, *Biosci. Biotechnol. Biochem.* 70 (2006) 1839.
- [77] L-N. Lin, A.B. Mason, R.C. Woodworth, J.F. Brandts, *Biochemistry* 33 (1994) 1881.
- [78] P.D. Jeffrey, M.C. Bewley, R.T.A. MacGillivray, A.B. Mason, R.C. Woodworth, E.N. Baker, *Biochemistry* 37 (1998) 13978.
- [79] J.W. Donovan, C.J. Mapes, J.G. Davis, J.A. Garibaldi, *J. Sci. Fd Agric.* 26 (1975) 73.
- [80] W.R. Harris, D. Nasset-Tollefson, J.Z. Stenback, N. Mohamed-Hani, *J. Inorg. Biochem.* 38 (1990) 175.
- [81] Y. Desfougères, A. Saint-Jalmes, A. Salonen, V. Vié, S. Beaufils, S. Pezenec, B. Desbat, V. Lechevalier, F. Nau, *Langmuir* 27 (2011) 14947.

## Figure captions

**Fig. 1.** Surface pressure ( $\Pi$ ) versus surface concentration ( $\Gamma$ ) for the lowest subphase concentrations for which the surface pressure is initiated:  $1 \mu\text{g.mL}^{-1}$  for ovotransferrin in citrate (open squares) and  $3 \mu\text{g.mL}^{-1}$  in acetate (filled circles). The insert in the BAM pictures ( $430 \times 540 \mu\text{m}^2$ ) shows the images of the surface for a pressure equal to  $0 \text{ mN.m}^{-1}$  and  $4 \text{ mN.m}^{-1}$

**Fig. 2.** Adsorption kinetics followed by ellipsometry measurements during 40 hours for a bulk concentration of  $100 \mu\text{g.mL}^{-1}$  at pH 4.0 in citrate (open squares) and acetate (filled circles). The shaded area corresponds to the variability of 11 kinetics obtained for the ovotransferrin in citrate.

**Fig. 3.** Surface pressure versus adsorption time (40 hours) for a bulk concentration of  $100 \mu\text{g.mL}^{-1}$  at pH 4.0 in citrate (open squares) and acetate (filled circles). Inset shows adsorption during 2 hours in citrate (open squares) and acetate (filled circles)

**Fig. 4.** Amplitude of the rotational motion of the float as a function of excitation pulsation, measured 20 h after the beginning of the adsorption of ovotransferrin at a bulk concentration of  $100 \mu\text{g.mL}^{-1}$  in citrate (a) and acetate (b)

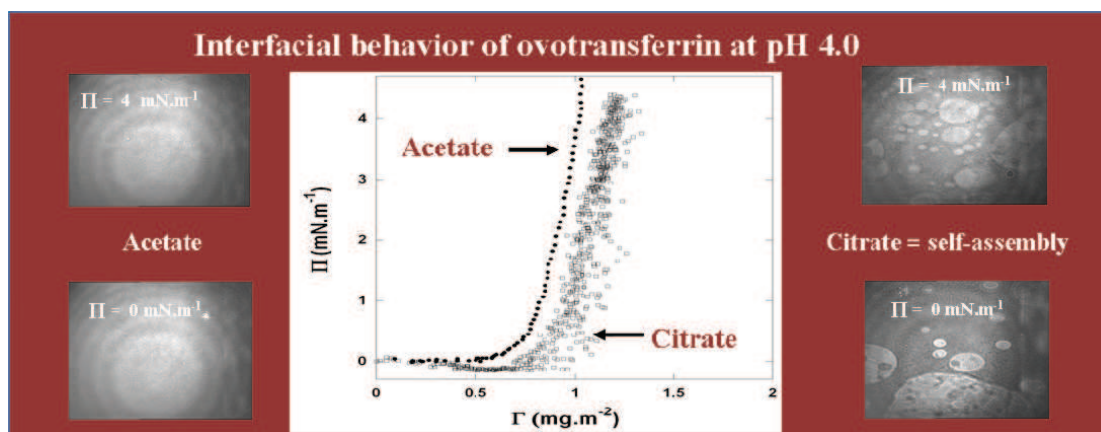
**Fig. 5.** Far- (a) and near- (b) UV CD-spectra of ovotransferrin in citrate (open squares) and in acetate (filled circles) at pH 4.0

**Fig. 6.** DSC scans on ovotransferrin in citrate (lower trace) and in acetate (upper trace) at pH 4.0. For clarity, DSC traces in this figure have been arbitrarily shifted on the ordinate scale



## Graphical abstract

Interfacial measurements of ovotransferrin in citrate and acetate buffer: surface pressure versus surface concentration and BAM images of the surface.



**Research highlights**

- ▶ In the first steps of adsorption citrate favors interfacial self-assembly.
- ▶ Interfacial heterogeneity in the presence of citrate.
- ▶ In the presence of citrate the interfacial layer is not viscoelastic.
- ▶ Citrate slightly increases helical content and affects the tertiary structure.
- ▶ Citrate stabilizes ovotransferrin against thermal denaturation.